Desalination and Water Treatment
www.deswater.com

doi: 10.5004/dwt.2022.29039

277 (2022) 120–135
November

A bench-scale electrochemical peroxidation reactor performance on removal of organic pollutants from tannery industrial wastewater

Selvabharathi Gopal[a], Adishkumar Somanathan[b,*], RajeshBanu Jeyakumar[c], Carlos Fernandez[d]

[a]*Department of Civil Engineering, SSM Institute of Engineering and Technology, Dindigul – 624002, Tamil Nadu, India, Tel. +91-9962441301; email: selthi2003@gmail.com*
[b]*Department of Civil Engineering, Anna University, Regional Campus, Tirunelveli – 627007, Tamil Nadu, India, Tel. +91-9841339016; email: adishk2002@yahoo.co.in*
[c]*Department of Life Sciences, Central University of Tamil Nadu, Thiruvarur – 610005, Tamil Nadu, India, email: rajeshces@gmail.com*
[d]*Lecturer in Analytical Chemistry, Robert Gordon University, Aberdeen (UK), email: c.fernandez@rgu.ac.uk*

Received 29 April 2022; Accepted 13 October 2022

ABSTRACT

The aim of this study is to evaluate the performance of a novel laboratory scale electrochemical peroxidation (ECP) reactor using iron (Fe) electrodes (anode and cathode) for treatment of tannery wastewater. In order to minimize operating cost, the effects of operating parameters were determined, and response surface methodology was used to optimize the operating parameters. The operating parameters were initial pH 2.2–8.4, H_2O_2 dosage 0–0.02 g/L, Fe^{2+} dosage 0–0.005 g/L and current density 10–40 mA/cm^2. Under the optimum conditions, the ECP process revealed better performance in terms of chemical oxygen demand (COD) removal with an average value of 85% in contrast to 65% removal in electro-Fenton (EF) process. Analysis and comparison of the data revealed that ECP process delivered a better treatment performance than EF process, taking into account that the optimum electrolysis time and applied current density were considerably. Overall, these results confirmed that the novel ECP reactor using Fe electrodes can reduce the operating cost and be proposed as a pragmatic approach to remove maximum amount of colour, COD, and chromium(III) from tannery wastewater.

Keywords: Tannery wastewater; Electrochemical peroxidation; Iron electrodes; Central composite design; Colour removal; Chemical oxygen demand reduction; Electrical energy consumption

1. Introduction

Tanning industry has contributed significantly to exports of many leather goods such as shoes, apparels and personal consumer leather products. Currently India occupies the third place in the global production of leather among the industrialized developing countries in the world. However, tanning industries produce large amounts of wastewater in the sequence of complex chemical reactions and mechanisms, which is ranked as the highest pollutants among all the industrial waste. The tanning sector is one of oldest and fastest growing industries with 2161 tanneries that process about 500 kilo tonnes of hides and skins with yearly disposed tannery wastewater of approximately 9,420 × 10^3 m^3 [1,2].

Tanneries produce wastewater with pH in the range of 5.8–10.5, total suspended solids (526–2,865 mg/L), biochemical oxygen demand (100–2,906 mg/L), chemical oxygen demand (2,102–11,153 mg/L) and chromium (16–65 mg/L) in 30–35 L/kg of skin/hide processed [3]. Tannins are one of the refractory groups of chemicals used in tannery wastewater.

---

* Corresponding author.

Tannins have complicated chemical properties and they are made up of a variety of chemicals including phenol, formaldehyde, and melamine-based syntan as well as acrylic polymers [4]. However, tannery industries produce large amounts of wastewater and the unregulated discharge of tannery wastewater into natural water source raises contamination and leads to adverse health impacts, posing a significant environmental hazard as well as a serious industrial problem.

The disposal tannery wastewater from desired level which could be due to heavy load of organic and inorganic pollutants like biological oxygen demand (BOD), chemical oxygen demand (COD), suspended solids, chlorides, chromium and dissolved solids, as reported in an earlier research study [5]. Tannery wastewater is treated by physical, chemical or biological processes. Treatment of tannery wastewater using biological methods involves many tedious steps and leads to many problems due to its toxicity. There is inhibition of biological degradation due to chromium content and sulphide ions indicating the antibacterial activity. Conventional methods used for wastewater treatment are expensive and are not eco-friendly besides requiring high energy and large quantities of chemicals [6]. The increasing demand for eco-friendly technologies has forced researchers, scientists and leather industries to search for cost-effective alternatives. The hazardous nature of effluents necessitates their treatment in an eco-friendly manner and the adoption of an effective treatment technology [7]. Hence, there is a vital need for devising more efficient, low-cost wastewater treatment processes with the use of chemicals and improved energy utilization to achieve better removal efficiency of pollutants [8].

In recent years, there have been many developments in advanced oxidation processes using electrochemical technology. The electrochemical advanced oxidation process (EAOP) prevents and remediates environmental pollution; especially focusing on water streams [9]. EAOPs can be further classified into electrochemical oxidation, electro-Fenton, electrochemical peroxidation, sono-electro-Fenton process etc. Due to the easy setting up of equipment, ease of use, high oxidation capacity, high process rate, complete pollutant removal of organic and inorganic contaminants with minimal expense, and ability to be integrated with other treatment methods, EAOPs have gained a lot of publicity for their significant role in pollutant removal from industrial wastewater [10]. The operational parameters and removal efficiencies of various EAOPs from different types of wastewater are shown in Table 1. Among the different EAOPs, the most recent development is the electrochemical peroxidation (ECP) system which is a composite approach that combines the Fenton and coagulation methods [11], it has been shown to be the proven method for removing pollutants and has been successfully deployed in the electroplating and dye industries [12]. The ECP is a variation of the electro-Fenton method in which a Fe electrode serves as a sacrificial anode for the electro-generation of Fe^{2+} ions and H_2O_2 is applied to the treated wastewater externally. The by-products obtained are Fe^{3+} ions which are the resultant of Fe^{2+} ions with hydrogen peroxide due to the applied DC current [13–15].

This catalyses the process due to the recycling of ferric ions into ferrous ions and offers a greater advantage than other ECP processes [16]. The ferrous species is continuously generated in the electrochemical cell that is responsible for the electrocoagulation of organic matter. Both H_2O_2 and Fe^{2+} ions are applied to the solution externally in this experiment; the ferrous ion (Fe^{2+}) interacts with H_2O_2 to form $OH^\bullet$, as seen in Eq. (1). The following equations describe the key reactions of the ECP process. Eq. (1) shows that the sacrificial iron anode releases Fe^{2+} ions into the solution Eq. (2).

$$Fe^{2+} + H_2O_2 \rightarrow Fe^{3+} + OH^- + OH^\bullet \tag{1}$$

The continuous replication of Fe^{2+} from Fe^{3+} that occurs at the cathode is seen in Eq. (3).

$$Fe \rightarrow Fe^{2+} + 2e^- \tag{2}$$

$$Fe^{3+} + 3e^- \leftrightarrow Fe^{2+} \tag{3}$$

Some hydroxyl radicals can react with Fe^{2+} and H_2O_2 during the process, resulting in $HO^\bullet_2$. As seen in Eqs. (4) and (5), this is not quite feasible in the oxidation phase that leads to quantification of H_2O_2 and Fe^{2+} [6]. According to Eq. (1), the ferrous ion (Fe^{2+}) formed by electrooxidation of the iron anode is precipitated as $Fe(OH)_3$, which is then self-oxidized to ferric (Fe^{3+}) ion in Eq. (6). As seen in Eq. (1), the formed $OH^\bullet$ radicals oxidise the organic compounds (RH) and convert them to H_2O and CO_2 as given in Eq. (6).

$$Fe^{3+} + OH^\bullet \rightarrow Fe^{3+} + OH^- \tag{4}$$

$$H_2O_2 + OH^\bullet \rightarrow HO_2^\bullet + H_2O \tag{5}$$

$$R - H + OH^\bullet \rightarrow \text{intermediates} \rightarrow H_2O + CO_2 \tag{6}$$

However, when comparing EAOPs to traditional treatment methods, one must regard power consumption as a critical parameter in EAOPs, in addition to pollutant removal performance [17]. Table 1 show that there is relatively little literature on the potential use of the ECP method for removal of the pollutants. The present research study is based on the ECP method using iron electrodes for colour, COD, and chromium(III) removal efficiency with minimal electrical energy consumption. The study also focuses on the optimisation of process parameters such as pH, H_2O_2 dosage, Fe^{2+} dosage, and current density using response surface methodology (RSM).

2. Methods and materials

2.1. Collection and characterization of tannery wastewater

Tannery wastewater was obtained from a small tannery industry located near Dindigul, Tamil Nadu, and India. All ECP experiments were carried out on the campus of University VOC College of Engineering, Anna University Thoothukudi campus, Thoothukudi, India (Latitude: 10° 22′ 8.26″ N Longitude: 77° 58′ 49.30″ E). After the plain sedimentation process, the sample was collected and stored at 4°C in a laboratory. Standard procedures were used to

Table 1
Operational parameters and removal efficiencies of various EAOP process from various wastewater

Type of wastewater	Initial COD (mg/L)	Operational parameters				Removal (%)	References
		pH	H_2O_2	Current density	Time		
Landfill leachate	5,500	3	300 mg/L	0.30 A/dm^2	240 min	97	[17]
Dyes wastewater	7,500	3	0.50 mM	66.7 mA/cm^2	360 min	85	[29]
Industrial wastewater	8,000	4	3.3 g/L	90 mA/cm^2	240 min	65	[7]
Vermiculite	Sodium vermiculite	3	0.150 mM	33.3 mA/cm^2	360 min	85	[8]
Photoelectrochemical wastewater	CSA, PANI-WO_3-rGO	–	130 mg/L	1.54 mA/cm^2	300 min	60	[31]
Lime wastewater	7,475	–	–	25 mA/cm^2	240 min	92	[22]
Sunflower oil refinery wastewater	6,500	6.5	–	11.56	400 min	90	[9]
Sugar beet industry process wastewater	13,500	5.3	21 mL/L	48.5	400 min	65	[46]
Canola oil refinery effluent	6,500	4	150 mg/L	13.66	7 h	85	[47]
Tannery wastewater	2,400	2.3	0.015 g/L	30 mA/cm^2	300 min	85	The present study

determine characteristics of the samples such as pH, COD, BOD, and total suspended solids [18]. The imhoff cone apparatus was used to determine the volume of sludge. The characteristics of the tannery wastewater were noted to be, pH = 7.5 ± 0.5, chemical oxygen demand = 2,370 ± 70 mg/L, biological oxygen demand = 985 ± 15 mg/L, colour (λ_{max} 465 nm) = 0.98 ± 0.100, chromium(III) = 16 ± 0.1 mg/L, total solids = 15,250 ± 200 mg/L, chloride = 510 ± 10 mg/L and electrical conductivity = 17,840 ± 1,500 µ/cm.

2.2. Chemical reagents

In this research, systematic studies were done to develop an effective treatment system with ECP process for treating tannery wastewater. The tests were carried out with ferrous sulfate heptahydrate [$FeSO_4{\cdot}7H_2O$] reagent grade hydrogen peroxide (H_2O_2) (30%, v/v). Sulfuric acid (H_2SO_4) and sodium hydroxide (NaOH) were used for the pH adjustment. Sodium thiosulfate (Na_2SO_3), potassium dichromate ($K_2Cr_2O_7$), mercuric sulfate ($HgSO_4$) and ferrous ammonium sulfate [$Fe(NH_4)_2(SO_4){\cdot}6H_2O$] were used for COD analysis. Sodium sulfate (Na_2SO_3) was utilised for quenching the reaction and all other reagents were procured from Merck (India). Deionized water was used to make various concentrations of solutions for all of these experiments.

2.3. ECP reactor and procedure

The ECP process was used to study the degradation of tannery wastewater at the University VOC College of Engineering, Anna University and Thoothukudi campus in Thoothukudi. A bench-scale reactor was made using acrylic material and a hopper bottom with the dimensions of 21.5 cm × 15 cm × 25 cm and capacity of 5 L was used to carry out the ECP process. The photographic view of the ECP experimental reactor is shown in Fig. 1. For the ECP process, both the cathode and anode were made of iron plates (218 cm^2). To prevent the experimental process from deteriorating, the electrodes were cleaned with emery paper (No. P320) and then washed with H_2SO_4 solution (5% v/v). The reactor was engraved with grooves to ensure a spacing of 6 cm between the electrodes. DC power supplies connected to the electrodes (0–30 V, 0–5 A) provided the desired current. The initial pH of the solution was controlled to the desired values with concentrated H_2SO_4 or NaOH. During each run, a predetermined amount of ferrous sulfate heptahydrate and hydrogen peroxide were applied to the reactor to active Fenton's reaction. Before the electrical current was switched on, 5 mL samples were taken every 10 min, and the pH was immediately changed with NaOH and sodium sulphite, to quench the production of $OH^{\bullet}$ discontinue the oxidation process and enable the residual iron to precipitate well (OR) which quenched the production of $OH^{\bullet}$, discontinued the oxidation process and

Fig. 1. Photograph view of electrochemical peroxidation reactor.

enabled the residual iron to precipitate well. The samples were allowed to settle for 30 min to allow for coagulation, after which the supernatant was taken for measurements [18]. Eqs. (7) and (8) were used to measure the colour and COD removal efficiencies, respectively (8).

$$\text{Efficiency of colour removal} = \frac{\left(A - A_t\right)}{A \times 100} \tag{7}$$

where A and A_t are the absorbance of tannery wastewater at the corresponding wave length ($\lambda_{\max}$ @465 nm) before and after removal absorbance of colour respectively.

$$\text{Efficiency of COD removal}\left(\%\right) = \frac{\left(\text{COD} - \text{COD}_t\right)}{\text{COD} \times 100} \tag{8}$$

where COD and COD_t are the chemical oxygen demand (COD) of wastewater before and after treatment, respectively. Electrical energy consumption is used as a parameter to measure the performance of the ECP processes. The estimation of energy consumption in kWh/L during removal efficiencies is shown in Eq. (9).

$$\text{Electrical energy consumption} = \frac{\left(\text{VIt}\right)}{V_S} \tag{9}$$

where kWh/L is electrical energy consumption, V is cell voltage in volts (V), I represents current in amperes (A), t is time (h), and V_S is volume of solution (L).

2.4. Response surface methodology and experimental design

The experimental design was optimised with the software Design-Expert version 8.0 to model the removal process, and response surface technique was used to reduce the experimental runs. Central composite, Box–Behnken, and D-optimal response surface designs are the most commonly used response surface method designs. The central composite design (CCD) was chosen for the current study. The design points on a CCD are divided into three categories: factorial design points, axial points ("star" points), and middle points. A quadratic model's coefficients are estimated using CCDs. Both point definitions will be in terms of factor coded values. The answer (output variable) will be optimised by careful experiment design determined by multiple input variables. The experiment is actually a sequence of experiments, known as runs, in which input variables are changed to determine the causes of differences in the output response. The response can be graphically interpreted in three-dimensional space or as contour plots that visualise the response surfaces [19]. In this study, there were four independent variables viz. pH 2.2–8.4, Fe^{2+} dosage 0 to 0.005 g/L, H_2O_2 dosage 0 to 0.02 g/L and current density. The range of the parameters was fixed by performing preliminary runs with current densities ranging from 10 to 40 mA/cm². It was used to determine the relationship between the ECP process responses (COD, colour removal and EEC) with the most important variables (pH, Fe^{2+} dosage, H_2O_2 dosage and current density). The following second-order mode Eq. (10) describes the relationships between the responses and process variables.

$$Y = \beta_0 + \sum_{i=1}^{k} \beta_i x_i + \sum_{i \le j} \beta_{ij} x_i x_j + \sum_{j=1}^{k} \beta_{jj} x_j^2 + \varepsilon \tag{10}$$

where Y is the response, β_0 is a constant coefficient; β_j, β_{jj} and β_{ij} are linear, quadratic and interactive effects coefficients, respectively; x_i and x_j are coded levels for the independent variables; k is the number of independent variables and ε is the random error.

3. Results and discussions

3.1. Statistical design and modelling using RSM

The values of the operating parameters of the ECP process determine the process efficiency. The parameters governing the ECP process in the current study were pH, H_2O_2 dosage, Fe^{2+} dosage, and current density. A set of 30 experiments was designed to optimize results which are summarized in Table 2. The operating parameters are interconnected with each other and affect the process efficiency significantly. For tannery wastewater treatment, good-fitting prediction models for representing COD, colour removal, and minimum EEC after removing negligible coefficients are discussed below in Eqs. (11)–(13).

$$\begin{aligned}\text{Colour removal}\left(\%\right) &= 83.88 - 2.52A + 3.30B + 4.08D - 4.49\text{AB} \\ &\quad - 4.03\text{AD} - 2.10\text{BC} - 10.56A^2 - 11.54B^2 - 11.13D^2\end{aligned} \tag{11}$$

$$\begin{aligned}\text{COD removal}\left(\%\right) &= 81.16 - 2.97A + 3.25B + 4.36D - 4.51\text{AB} \\ &\quad - 3.87\text{AD} - 2.42\text{BC} - 1.21\text{BD} - 8.09A^2 - 10.45B^2 - 15.03D^2\end{aligned} \tag{12}$$

$$\begin{aligned}\text{EEC} &= 0.014 + 8.944E - 004A - 1.461E003B + 6.000E + 7.889 \\ &\quad - 004D - 4.687E - 1.781E - 003\text{AC} - 6.937E - 003\text{BC} \\ &\quad + 9.812E - 5.116E - 003A^2\end{aligned} \tag{13}$$

The extent of colour removal can be seen in Eq. (11). The independent variables *A*, *B*, *D* as well as the interaction variables *AB*, *AD*, *BC* were important model terms. Other model terms were insignificant as the possibility significance was higher than 0.05. It was concluded from the positive linear coefficient that the operational parameters like pH, Fe^{2+} and current density influence the colour removal efficiency. However, according to the negative coefficient, an inhibitory effect was observed with the values of H_2O_2. In the COD removal, shown by Eq. (12), the test variables *A*, *B*, *D*, *B*, *AD*, *BC*, and *BD* were the significant model terms [20]. The test variables *A*, *B*, *D*, *BC* and *CD* were the important model terms for the electrical energy consumption as shown in Eq. (11).

3.2. Analysis of variance and interactive effects of parameters

In order to determine the adequacy of the model some assessments are needed for regression model deliberation. Statistics such as *F*-values, *P*-values and *R*-squared are used for comparing the models. Table 3 shows the findings of the analysis of variance (ANOVA). The coefficient repeats the goodness of fit for the model (*R*). When R^2 is similar to 1, the model will forecast the response, and when $R^2 > 0.98$, R^2 adjusted > 0.96, and R^2 predicted > 0.93 for all responses, the regression model qualifies the investigational values and provides an excellent explanation of association with the independent variable and responses [21].The model was deemed to be statistically significant because the Prob. > *F* (*P*-values) values from the ANOVA were less than 0.05. The values of Prob. > *F* were 0.0001 in all of the models used in this study. Fischer's F-statistics values (*F*-values) for colour loss, COD removal, and electrical energy consumption were 876, 839, and 55, respectively. The coefficient of variance (CV), defined as the ratio of the standard error of estimate to the mean value of the observed response (as a percentage), was used to assess the model's reproducibility, with a CV of less than 10% being considered reproducible. The model was found to be sufficiently reproducible based on the values of CV, as seen in Table 3. For all reactions, a *P*-values greater than 4 mean a sufficient signal. For the responses, the higher the *F*-values and the lower the *P*-value, the more likely the regression model will explain the majority of the variance in the responses [22]. As a result of the foregoing evidence, the quadratic model can be used to follow the CCD-defined design space for the ECP mechanism. It is, however, critical to specify a suitable hypothetical distribution for random variables. Interfering with coefficient of variance values leads to the conclusion that the model is feasible and reproducible. When the AP value is greater than 4 it means that there are enough signals for all responses.

The response variables of colour and COD removal with minimum EEC were represented individually in a three-dimensional graph by varying every two of four input parameters. A total of six numbers of three-dimensional graphs were plotted for each response variable for wastewater. From Table 1, RSM analysis for the responses (colour, COD and EEC) satisfied the norms and conditions; thence it was chosen to visualize the process performance. Similarly, the Box–Cox plot, normal probability and the residual plots which interconnect the experimental and predicted values are shown in Fig. 2. Through the curvature of the three-dimensional surfaces, it was observed that a few interactions among factors were critical. The optimal conditions for most extreme estimations of the responses were ascribed to all factors: pH, Fe^{2+}, H_2O_2 and current density.

3.3. Interaction of operational variables

3.3.1. Interactive effectof pH

The performance of the ECP process for the degradation and decolourization of tannery wastewater was studied at

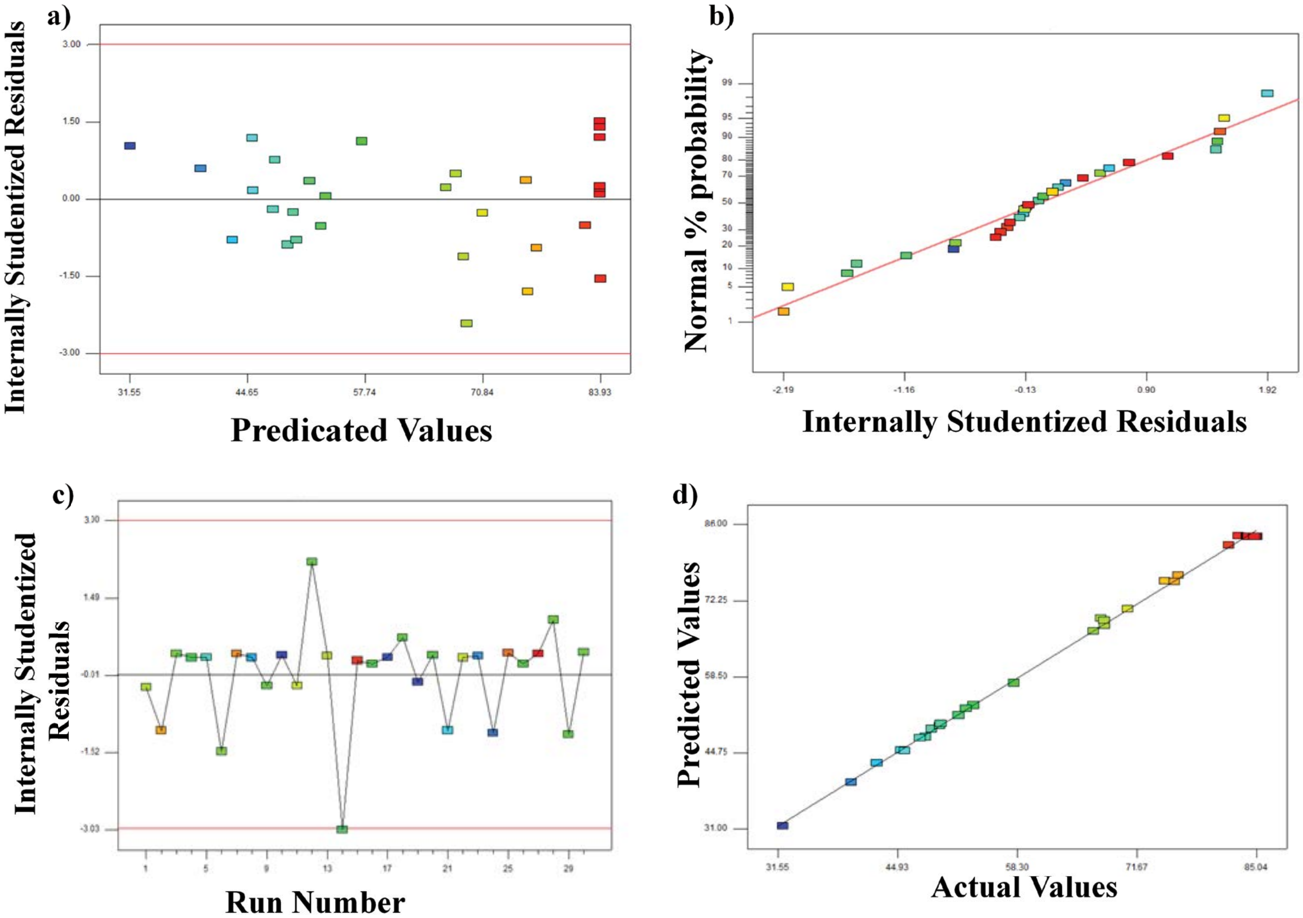

Fig. 2. (a) Box–Cox plot, (b) normal probability plot of residuals, (c) plot of residuals vs. run number and (d) actual values vs. predicted values.

pH 2.2–8.4. The contour map and response surface of various factors affecting pH as shown in Fig. 3. The obtained outcome shows that pH is a relevant operating variable that affects the generation of hydroxyl radicals and ferrous ion complexes, as well as iron speciation and H_2O_2 decay [23]. From Table 2, it can be seen that the highest removal efficiency of 83% of colour and 81% of COD with 0.077 kWh/L electrical energy consumption were achieved at pH = 2. The effect of pH on colour, COD removal and EEC is represented in Fig. 4. Since ferric ions (Fe^{2+}) are water soluble and play a catalytic function in the production of $OH^{\bullet}$, the ECP treatment method was enhanced. At pH 2, iron species form stable complexes with H_2O_2, causing catalyst deactivation and a reduction in removal efficiency, as given in Eq. (13). H_2O_2 cannot be disintegrated to $OH^{\bullet}$ by Fe^{2+} at pH 2. By arresting one proton, H_2O_2 transforms into $H_3O_2^+$ in ECP. Since $H_3O_2^+$ is electrophilic, the reaction rate between H_2O_2 and Fe^{2+} is slow [24], thus decreasing the treatment efficiency. When pH value increases from 2, it affects the ECP process and it invariably reduces the removal efficiency due to the transformation of ferrous ions into ferric ions, as given in Eqs. (14) and (18), and in succession to ferric hydro complexes or ferric oxyhydroxide. In addition, ferric ions can form $Fe(OH)_3$ which will not react with H_2O_2 and consequently, decrease the removal efficiency [25].

$$H_2O_2 + H^+ \rightarrow H_3O_2^+ \tag{14}$$

$$HO_2 + Fe^{2+} \rightarrow HO_2^- + Fe^{3+} \tag{15}$$

$$Fe^{2+} + HO^{\bullet} \rightarrow Fe^{3+} + OH^- \tag{16}$$

$$Fe^{3+} + H_2O_2 \rightarrow FeOOH^{2+} + H^+ \tag{17}$$

$$Fe^{2+} + 2OH^- \rightarrow Fe\left(OH\right)_2 \tag{18}$$

Concentration of chromium(III) reduced from 16 to 2.6 mg/L (87%) as inferred from Cr(III) precipitated as chromium hydroxide. The organic pollutants were degraded and the highest degradation was obtained at pH 2.1. Electrical energy consumption was not significantly affected by pH = 2.

3.3.2. Interactive effect of Fe^{2+}

The effect of Fe^{2+} (0 to 0.005 g/L) on the degradation of tannery wastewater in ECP was investigated. The contour map and response surface of various factors affecting Fe^{2+} observations are shown in Fig. 5. Since Fe^{2+} is superior to Fe^{3+}, a sufficient Fe^{2+} concentration is necessary for the initiation of Fenton's reaction to dissolve large molecules in real wastewater than synthetic wastewater [26]. Ferrous salts are added to achieve metal coagulation until the concentration stays elevated and is adequate enough to degrade the contaminants [27]. If Fe^{3+} species are present in the medium, they are reduced to Fe^{2+} by reducing H_2O_2 or organic intermediate radicals, as given in Eq. (19), or by direct Fe^{3+} reduction on the surface.

$$Fe^{3+} + H_2O_2 \rightarrow Fe-OOH^{2+} \rightarrow Fe^{2+} + H^+ + HO_2^{\bullet} \tag{19}$$

Fig. 6 shows that the absence of Fe^{2+} dosage resulted in the removal efficiency becoming 67%. This is because the oxidising ability of hydrogen peroxide is insufficient to dissolve massive molecules in the absence of ferrous ions. In the presence of Fe^{2+}, the ECP process with high efficiencies reduces colour and COD more effectively [28].

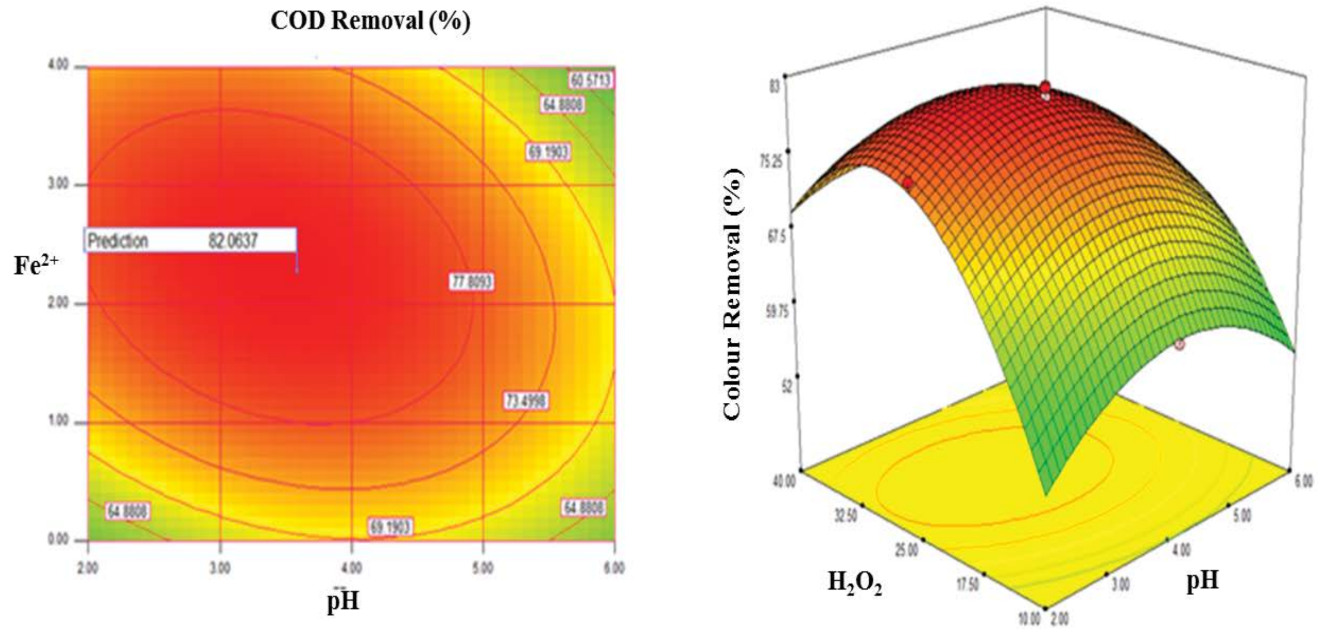

Fig. 3. Contour map and response surface of various factors affecting pH.

Table 2
Experimental conditions and its results of CCD design for ECP process

Run	Factor 1	Factor 2	Factor 3	Factor 4	Responses		
	pH	Fe^{2+} (g/L)	H_2O_2 (g/L)	Current density (mA/cm^2)	Colour removal (%)	COD removal (%)	Electrical energy consumption (kWh/L)
1	4	0.002	0.025	25	83.03	79.91	0.0156
2	2	0	0.025	40	57.91	53.84	0.0174
3	4	0.002	0.015	10	68.03	61.32	0.0148
4	6	0.004	0.005	10	48.68	43.95	0.014
5	2	0	0.005	40	49.71	46.16	0.0111
6	6	0	0.005	10	45.32	39.22	0.015
7	4	0	0.015	25	67.64	68.42	0.0177
8	8	0.002	0.015	25	70.65	68.76	0.0098
9	4	0.004	0.015	25	75.86	72.6	0.0145
10	2	0	0.005	10	32.04	27.12	0.008
11	4	0.002	0.015	40	76.29	70.54	0.0161
12	2	0.004	0.025	40	66.83	62.33	0.0144
13	8	0	0.025	40	51.71	47.61	0.0157
14	4	0.002	0.015	25	84.05	81.07	0.0121
15	2	0	0.025	10	39.71	35.62	0.0187
16	4	0.002	0.015	25	83.96	81.45	0.014
17	2	0.004	0.005	10	53.38	51.05	0.0082
18	4	0.002	0.015	25	84.08	80.94	0.0143
19	2	0.002	0.015	25	74.81	76.98	0.0078
20	4	0.002	0.015	25	85.04	80.84	0.0141
21	2	0.004	0.025	10	52.57	47.79	0.0104
22	6	0	0.005	40	48.02	44.01	0.016
23	8	0.005	0.025	10	45.71	41.38	0.0096
24	6	0.004	0.025	40	42.57	38.67	0.0091
25	6	0.005	0.005	40	47.38	43.22	0.018
26	4	0.002	0.015	25	84.96	82.04	0.014
27	8	0	0.025	10	49.58	45.35	0.0193
28	4	0.002	0.015	25	84.81	81.77	0.0145
29	2	0.004	0.005	40	68.07	64.82	0.0144
30	4	0.002	0.005	25	81.96	78.32	0.0147

Table 3
Analysis of variance (ANOVA) for the fitted polynomial model

S. No.	Source	Colour removal	COD removal	Electrical energy consumption
1	Standard deviation	0.81	0.86	0.0006163
2	Mean	63.48	59.90	0.014
3	*R*-squared	0.9988	0.9987	0.9811
4	Adj. *R*-squared	0.9976	0.9975	0.9634
5	Pred. *R*-squared	0.9955	0.9934	0.9330
6	PRESS	36.57	57.89	0.000020
7	Coefficient of variance (CV %)	1.28	1.44	4.47
8	Adequate precision	91.39	88.09	25.90
9	*F*-value	876.02	839.64	55.51
10	*P*-value	<0.0001	<0.0001	<0.0001

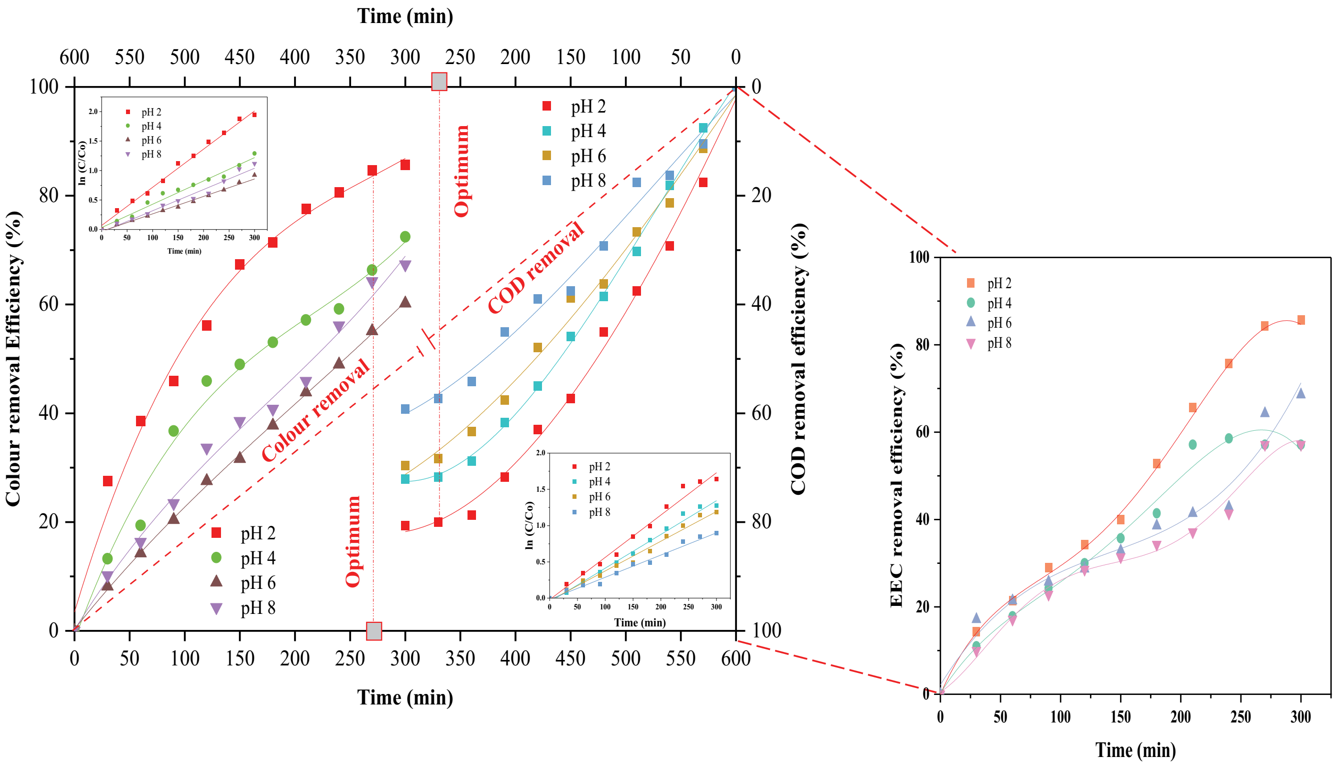

Fig. 4. Effect of pH on colour, COD removal and EEC.

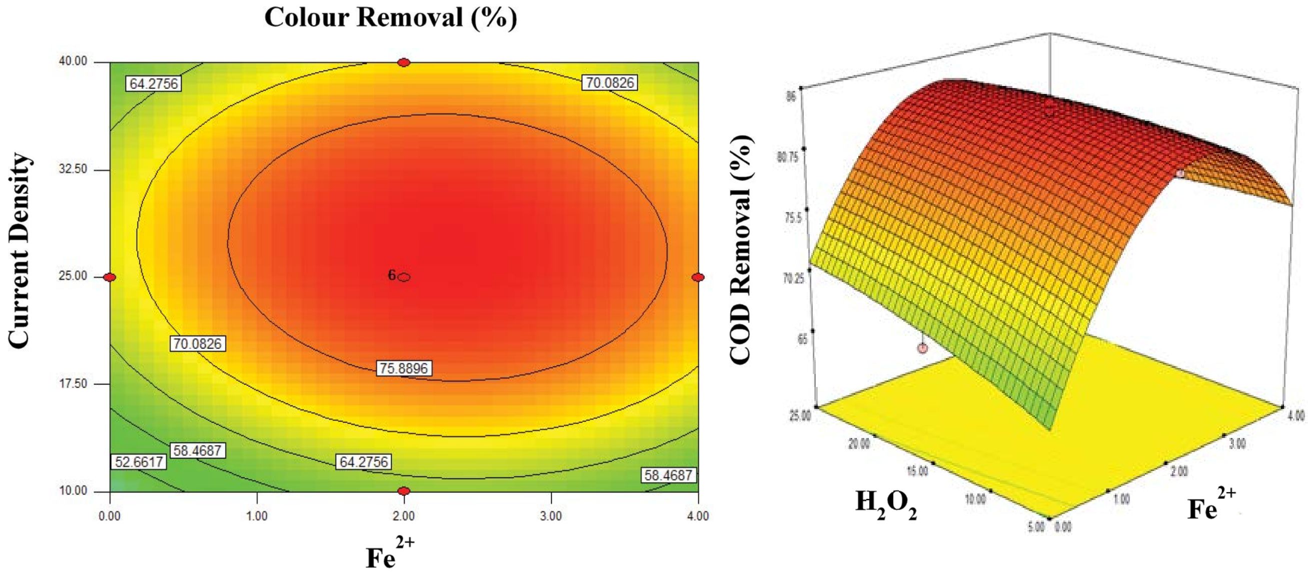

Fig. 5. Contour map and response surface of various factors affecting Fe^{2+}.

By increasing the amount of Fe^{2+} in a range varying from 0 to 0.002 g/L, the COD efficiency improved from 67% to 81%. Similarly, colour removal increased from 69% to 83% and EEC was minimized from 0.082 to 0.077 kWh/L. Thus, with the occurrence of Fe^{2+} deposits (iron electrodes), the generation of hydroxyl radicals is increased when H_2O_2 is present. By accepting a proton, this $OH^{\bullet}$ react with the organic compound [29]. The removal efficiency of Fe^{2+} dropped to 73% and 75% for COD with additional increase in Fe^{2+} dosage and colour, respectively, while the electrical energy consumption was minimised to 0.077 kWh/L. Therefore, when $Fe^{2+} > 0.002$ g/L, it had a negative impact on COD and colour removal efficiency [30] in succession to ferric hydro complexes or ferric oxyhydroxide, as given in Eq. (20).

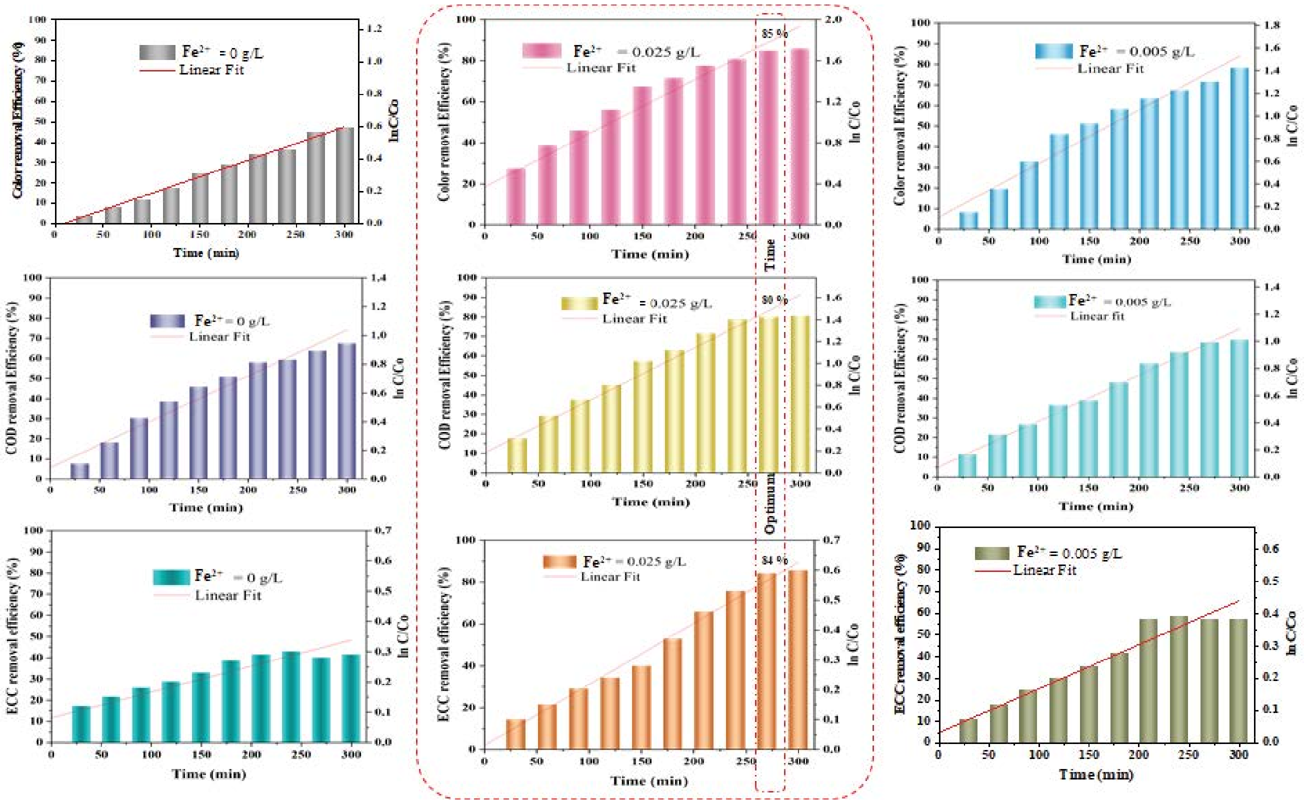

Fig. 6. Effect of Fe^{2+} on colour, COD removal and EEC.

$$Fe^{3+} + H_2O_2 \leftrightarrow FeOOH^{2+} + H^+ \quad (20)$$

As iron electrode was used as both anode and cathode, simultaneous breakdown of Fe^{2+} in the anode and regeneration of Fe^{2+} in the cathode occurred in the reactor. When Fe^{2+} dose exceeded the optimal amount of 0.002 g/L in the ECP phase, a scavenging effect of $OH^{\bullet}$ was observed. The increase in Fe^{2+} concentration from 0 to 2 mg/L resulted in an improvement in Cr(III) elimination from 40% to 86% and a decrease in Cr(III) concentration from 16 to 2.8 mg/L. The effect of Fe^{2+} on colour, COD removal and EEC is depicted in Fig. 6.

The enormous amount of foregoing Fe^{2+} can react with the useful hydroxyl radicals, resulting in a decrease in removal ability [31]. Furthermore, the $OH^{\bullet}$ released by Fe^{3+} oxidises into Fe^{2+}, trapping the presumed solids and resulting in the precipitation of metal hydroxides, which are accumulated as iron sludge, which adsorbs the dissolved pollutants [11,32]. According to Y. Wang et al. [48], when ferrous ions in electrolytes are present in excess, they absorb hydroxyl radicals and affect the degree of degradation. As a result, the best result was obtained at 0.002 g/L when the Fe^{2+} ions were prompted to produce hydroxyl radicals.

3.3.3. *Interactive effect of H_2O_2*

To address the excessive H_2O_2 accumulation, it is recommended that a desired amount of hydrogen peroxide be added to the ECP process. The degradation and decolourization of tannery wastewater were studied from 0 to 0.02 g/L to determine the effect of H_2O_2 dosage. Fig. 7 represents the contour map and response surface of various factors affecting H_2O_2. It was observed that the colour and COD removal efficiencies improved on increasing H_2O_2 dosage up to 0.015 g/L. This was because of the improvement of very reactive hydroxyl radical, the highest COD removal of 85% and Cr(III) removal of 86% in 240 min was achieved when 0.015 g/L of H_2O_2 was added to ECP. According to Eq. (21), the presence of H_2O_2 in ECP will result in the rapid generation of Fe, as given in Eq. (22) [33].

$$2H_2O_2 + 2e^- \rightarrow 2OH^- + H_2 \quad (21)$$

$$Fe^{2+} + H_2O_2 \rightarrow Fe^{3+} + OH^{\bullet} + OH^- \quad (22)$$

As seen in Fig. 8, in the absence of H_2O_2, the extraction efficiency of colour and COD was reduced by 78% and 72%, respectively. Where the amount of iron is greater than hydrogen peroxide, the Fenton reaction will use ferrous ion as a reactor. Since the coagulating properties were dominant during the removal of colour and COD by Fenton, the oxidation properties had little effect on the removal of this pollutant. This process will consume hydroxyl radicals formed by trivalent iron ions (Fe^{3+}) and oxidise them into bivalent iron (Fe^{2+}), resulting in the non-beneficial degradation of H_2O_2. As H_2O_2 dosage was increased from 0.015 to 0.02 g/L, the colour and COD removal efficiency dropped from 85% to 64%.

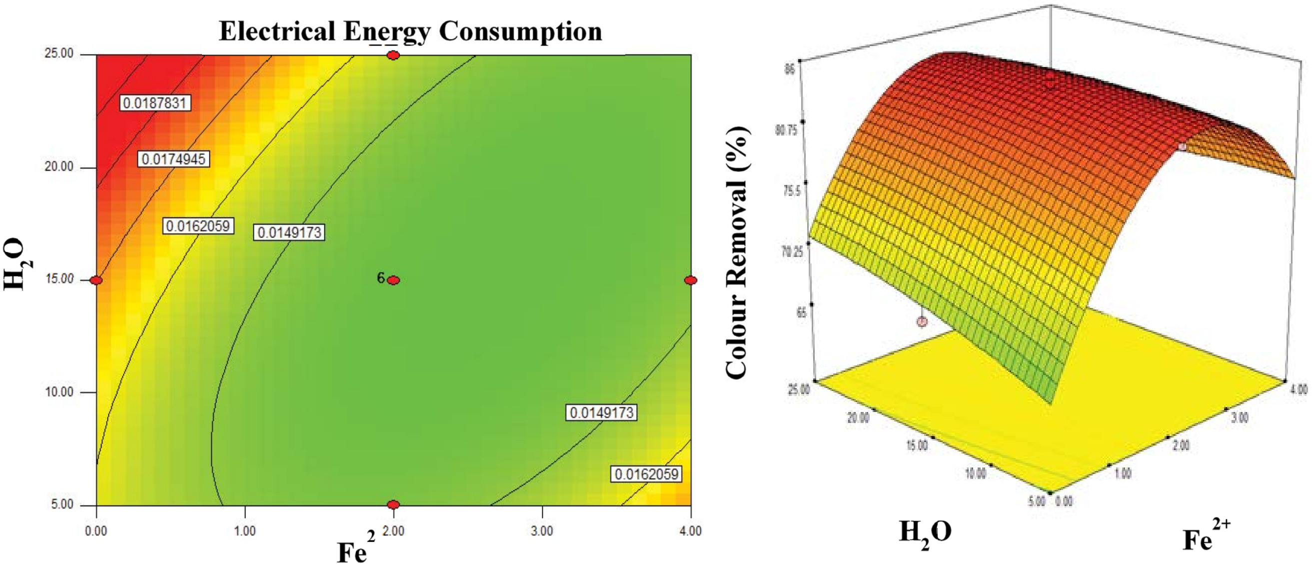

Fig. 7. Contour map and response surface of various factors affecting H_2O_2.

The explanation for this may be because hydrogen peroxide competes with organic pollutants for electrons, resulting in the depletion of ferrous ions in the solution [34]. Simultaneously, this reaction may be the result of reversible pollutant transfer. As a result of the hydrogen peroxide decomposition, the hydroperoxyl radical was formed; as seen in Eq. (23), this is a mild oxidant relative to the hydroxyl radical, resulting in slower degradation [35].

$$Fe^{2+} + H_2O_2 \rightarrow Fe^{3+} + OH^{\bullet} + OH^{-} \quad (23)$$

Thus, it is inferred that H_2O_2 dosage of 0.015 g/L promotes and shown the effect of H_2O_2 on colour, COD removal and EEC in Fig. 8.

3.3.4. Interactive effect of current density

Current density is one of the most critical parameters in the electrochemical peroxidation (ECP) method for regulating the reaction rate inside the ECP reactor, as its importance proves to be decisive in deciding operating cost and process performance in industries such as mineral production and textiles [36]. The contour map and response surface of various factors affecting current density as shown in Fig. 9. The tests were carried out at a current density of 10–40 mA/cm^2. As current density was increased from 10 to 30 mA/cm^2, colour and COD removal increased from 61% to 81%, 68% to 83%, and the EEC decreased from 0.083 to 0.077 kWh/L, respectively. This improvement in removal performance can be explained by the fact that increasing the electrical current between the iron electrodes causes the anode to dissolve more quickly, resulting in the formation of metal species [34–37]. The amount of dissolved iron ions, the formation of $Fe(OH)_3$ and current density determine the COD removal efficiency. Oliveira Marcionilio et al. [35] and Jing et al. [32] reported comparable findings, with current densities of 80 and 19.23 mA/cm^2. From 10 to 30 mA/cm^2, the rate of anode dissolution was directly proportional to the increase in current density. As a result, the number of metal hydroxide flocs increased, increasing Cr(III) removal performance from 40% to 86%. The applied current density acted as a stimulator, resulting in the generation of oxidised iron (Fe) at the anode and $OH^{\bullet}$ at the cathode via oxygen reduction. The developed Fe^{2+} interacted with H_2O_2 at the anode, generating hydroxyl radicals that helped to reduce the pollutants. The increase in Fe^{2+} concentration was identical to the increase in current density. The current density boosted the system's performance by raising the coagulant output rate (the volume of Fe^{2+} ions emitted by the anode), which influenced the growth of flocs in the ECP reactor [11]. As current density was stable, a fixed volume of Fe^{2+} was released in the solution, according to Faraday's law. The reduction and removal of COD and colour was relieved by the presence of ferrous ions. At a current density of 30 mA/cm^2, the drop in COD and colour removal from ECP caused further scarification of the anode, resulting in excess Fe^{2+} and a ratio of H_2O_2 to Fe^{2+} below the optimum level of 8. The effect of current density on colour, COD removal and EEC are shown in Fig. 10. From Fig. 10, it is seen that the optimal current density was30 mA/cm^2, and the measured electrical energy consumption was 0.077 kWh/L. Lozano et al. [38] discovered that different current density values influence cell voltage, which could be beneficial for COD removal. If the current density is poor, the lack of coagulant can limit the efficiency of removal.

3.4. Response optimization and recognition of the experimental design

An experiment was carried out at optimal conditions for tannery wastewater treatment in order to verify the projected versions. The experimental work was conducted under

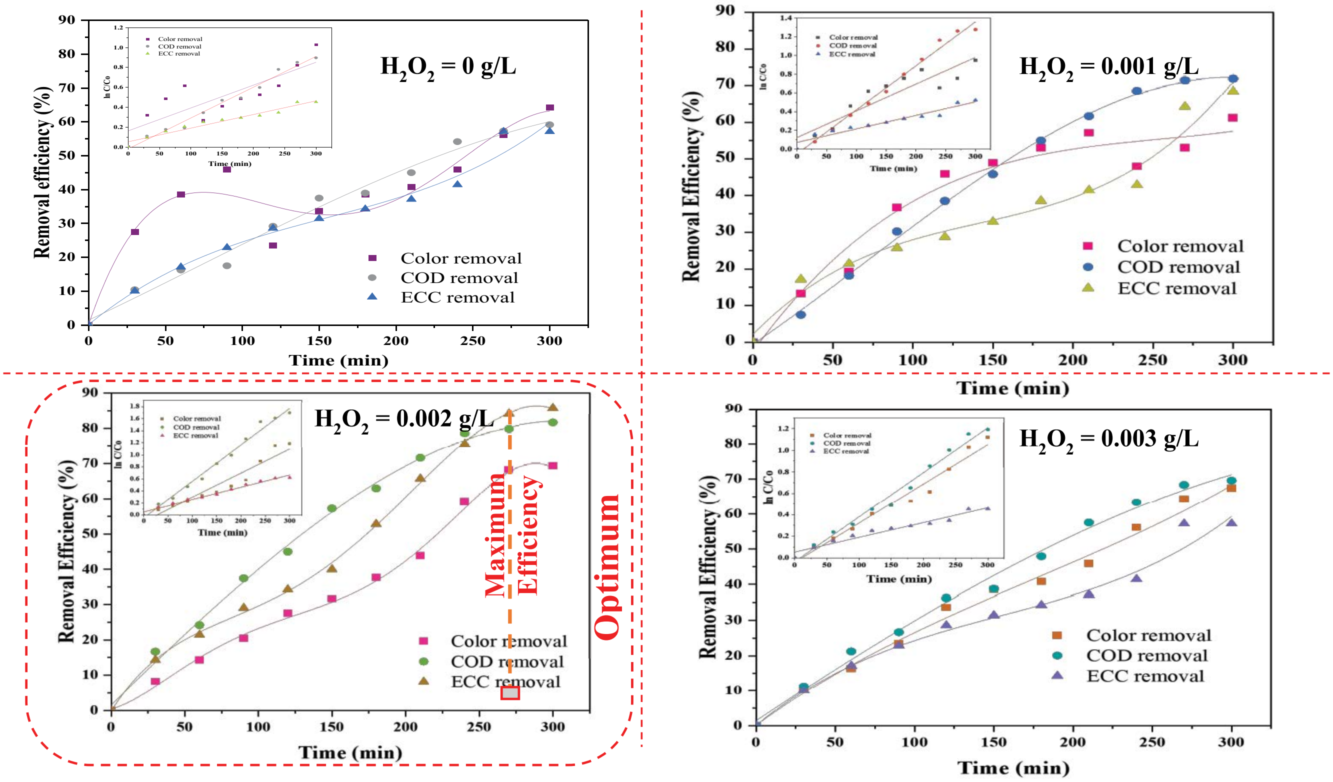

Fig. 8. Effect of H_2O_2 on colour, COD removal and EEC.

ideal conditions with the clear purpose of confirming the accuracy of the expected models, and the findings are presented in Table 4. The highest removal of colour, COD and corresponding electrical energy consumption were noted to be around 85%, 82% and 0.077 kWh/L, respectively, which were attained at pH = 2, Fe^{2+} = 0.002 g/L, H_2O_2 = 0.015 g/L, at a current density = 30 mA/cm^2 for the ECP process after optimizing the process using CCD and percentage of error in the predicted value was very less when compared to the observed value shown in Table 4. RSM is an important instrument for improving the operating conditions of the ECP method for COD and colour elimination, according to the experimental findings.

3.5. Electrical energy consumption

While determining the running expenses of the wastewater treatment process, it is important to consider the amount of electrical energy used in the ECP process. Fig. 9 shows the effects of determining the effective cut-off ECP reactor using optimal operating conditions over a range of time intervals (30–300 min). The initial operating time (30 min) of the process shows 0.049 kWh of EEC per kg of COD removal for 12%. The EEC and energy cost of the process gradually increased from 30 to 240 min corresponding to the different time intervals showing the increment in the COD removal from 12% (at 30 min) to 82% (270 min).The maximum COD removal with ECP reactor efficacy (82%) was obtained at 270 min of operation with 0.014 kWh/L whereas the cost of energy was 0.25 $/m^3. The electrical energy used for the ECP procedure was a major factor in the treatment's running costs [38]. However, by further increasing the current density, the EEC was raised from 0.014 to 0.0156 kWh/L, and the COD was reduced from 82% to 76% [24]. Treatment of dye wastewater by electrocoagulation (EC) and electro-Fenton (EF) provide the high removal efficiency and lower specific energy consumption 0.078 kWh/L [39]. In poultry wastewater, treatment of EF process turbidity 93% and COD 97% were decreased with 0.009 kWh/L of EEC [23]. Removal efficiency of COD rises from 31% to 98% with EEC increases from 2.59 to 8 kWh/m^3 for the treatment of landfill leachate wastewater [17]. The textile wastewater treatment by electrocoagulation, electrochemical Fenton, electro-Fenton and peroxi-coagulation of colour removal (93%) is increased in EEC 300 mA [34]. Treatment of heavy metals from simulated wastewater EEC from 4.43–75.71 kWh/kg under optimal condition [40,41].

These results showed that the current density must operate this range 10 to 40 mA/cm^2 achieve higher removal of pollutants along with minimum EEC for the ECP process to be economically viable. The electrochemical treatment techniques indicate the EEC in a future threat to be challenged in the nearby approaching is their combination with other techniques, whichever to source the cells with a renewable energy source or combination with solar radiation [7].

3.6. Effect of ferrous ions on the ECP process

In the ECP solution phase, iron concentrations are observed on the surface of the cathode, as seen below, and the use of iron electrodes leads to the formation of Fe^{2+} on

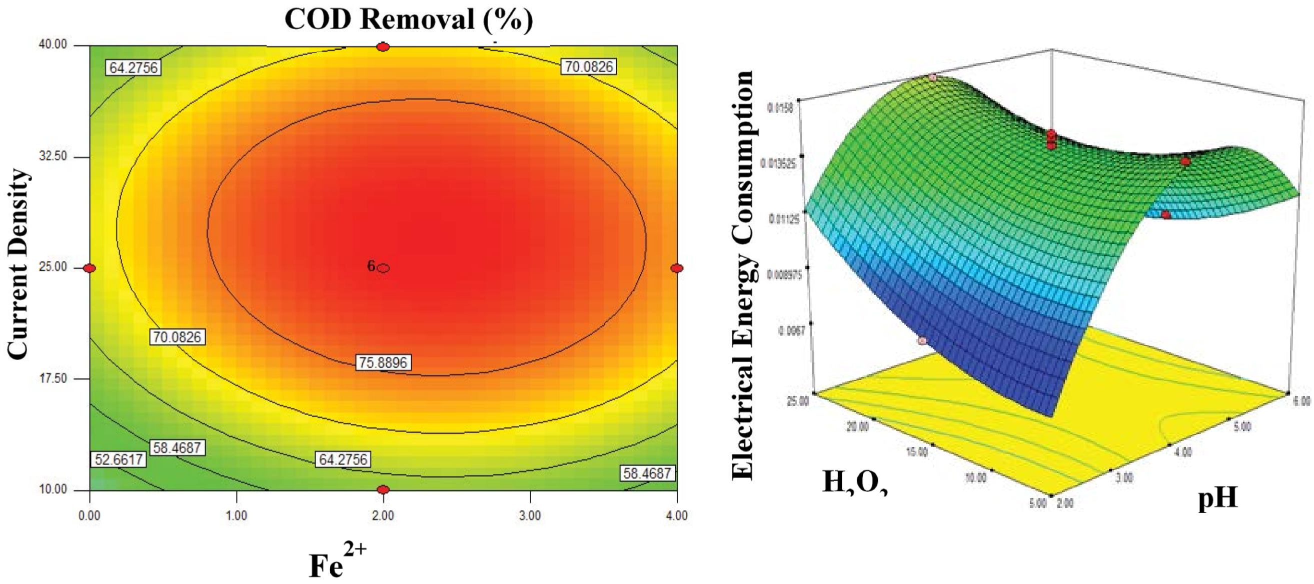

Fig. 9. Contour map and response surface of various factors affecting current density.

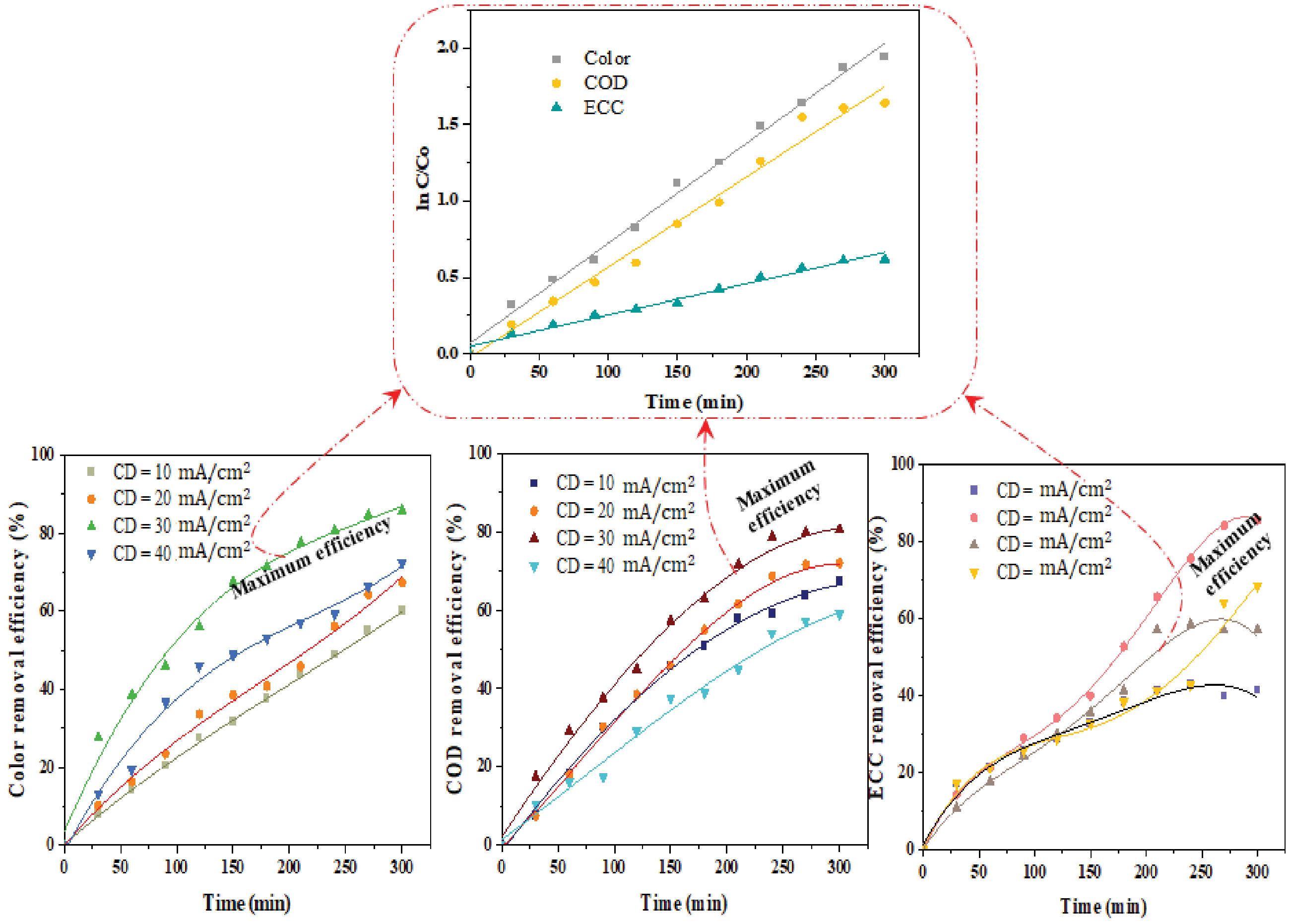

Fig. 10. Effect of current density on colour, COD removal and EEC.

Table 4
Response optimization and validation of the experimental design

S. No.	Parameters	pH	Fe^{2+} (g/L)	H_2O_2 (g/L)	Current density (mA/cm²)	Colour removal (%)	COD removal (%)	EEC (kWh/L)
1.	Predicted value	2	0.002	0.015	30	84	82	0.079
2.	Experimental value	2	0.002	0.015	30	85	82	0.077
3.	Error	–	–	–	–	+1.00	0.00	+0.002

the surface of the electrode. Eq. (24) uses Faraday's law to measure the amount of Fe^{2+} formed on the particle surfaces.

$$m = \frac{MIt}{nF} \tag{24}$$

When iron electrodes are used, there is an improvement in the reformation and synthesis of iron ions (Fe^{2+}). The amount of iron ions produced in the tannery wastewater needed to achieve the target stage was determined to be 230 mg [42]. External Fe^{2+} requirements were reduced as a result of the additional generation of iron ions, and hence the bulk of produced H_2 and created hydroxyl ions could be planned [43]. On the contrary, when the electro-Fenton process was applied, COD and Cr(III) removal only reached 62% and 60%, respectively. Despite the EF process carried out without addition of Fe^{2+}, the removal process exhibited lower efficiency and the results are as illustrated in Fig. 11. If there is an insufficiency of Fe^{2+} ions produced from electrodes, they react with H_2O_2, and lower colour (70%) and COD removal (62%) are obtained [44]. This leads to reduction in formation of $OH^•$ radicals which are not able to eliminate the impurities from wastewater [45].

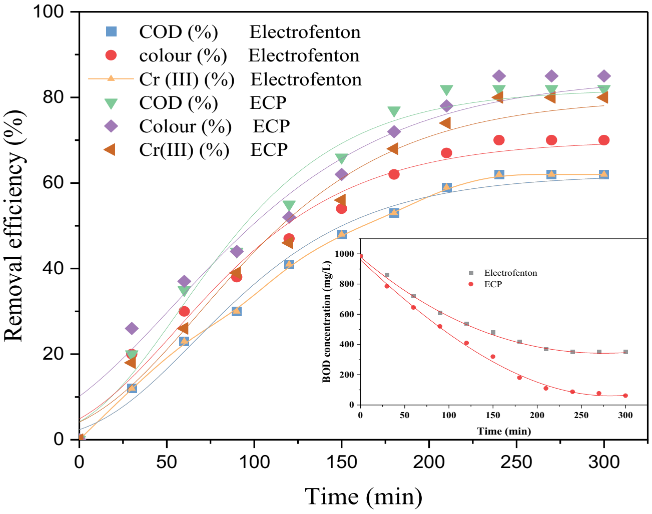

Fig. 11. Effect of ferrous ions on the ECP process.

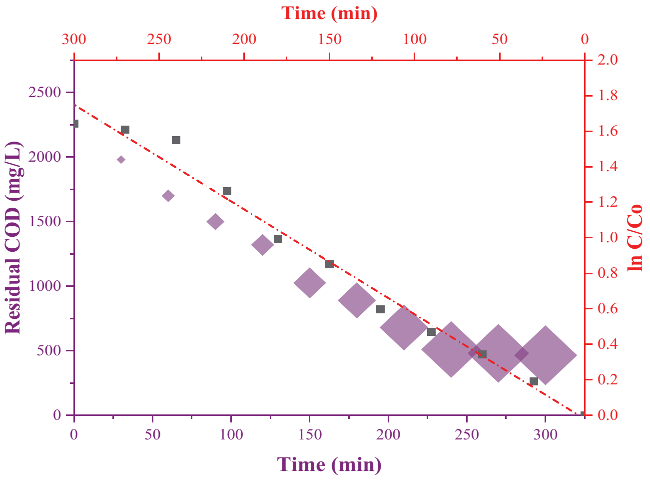

Fig. 12. Effect of contact time.

3.7. Influence of contact time

Experiments were carried out to determine the effect of time on the degree of total deterioration under optimum conditions. The decrease in COD with contact time is shown in Fig. 12, COD removal increased significantly with a reaction time of 150 min, varying from 20% to 60% for tannery wastewater, according to the results. The interaction time was increased from 30 to 300 min, which resulted in a steady change in COD removal, with around 82% of COD removed in 270 min. Since the experimental evidence tends to fit the linear kinetic equation, the removal efficiencies appear to first-order kinetics. ECP was the rate constant order (0.0423 min⁻¹) > EF (0.0041 min⁻¹). The ECP process was found to be 1.25 times faster than the EF process. The corresponding COD removals for each contact time were measured and are shown in Fig. 12. There was a noticeable reduction in colour and Cr(III) removal initially, up to 150 min, and then it remained at nearly the same level due to the formation of ferric complexes [46] when the time was increased, as shown in Fig. 12, COD, colour, and Cr(III) removal all increased significantly up to 150 min, with the COD value dropping to less than 435 mg/L, colour removal efficiency nearing 85%, and Cr(III) removal efficiency 85% for tannery wastewater. The removal of Cr(III) from tannery wastewater by ECP process is shown in Fig. 13. The ECP procedure was more effective in removing COD and increasing the biodegradability of the wastewater over time. For the purpose of evaluation, BOD samples were taken every 30 min under ideal treatment conditions. Fig. 14 shows the biodegradability of tannery wastewater improved from 0.3 to 0.63 after 300 min of contact time. The improvement of the characteristics of wastewater to a level of biologically degradable and increased biodegradability is shown by a higher BOD_5/COD

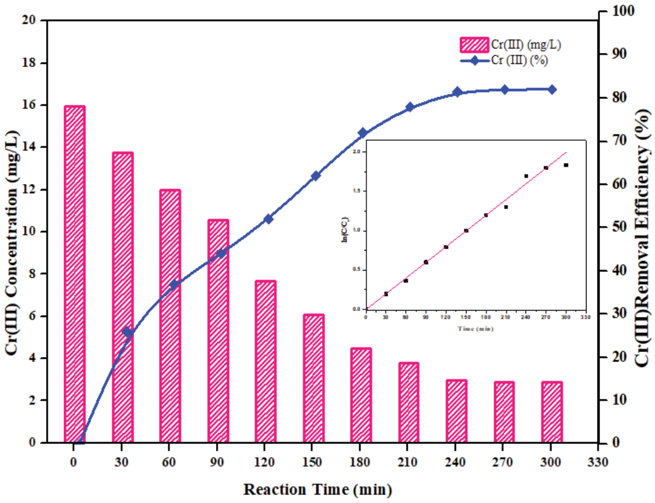

Fig. 13. Chromium(III) removal by ECP process.

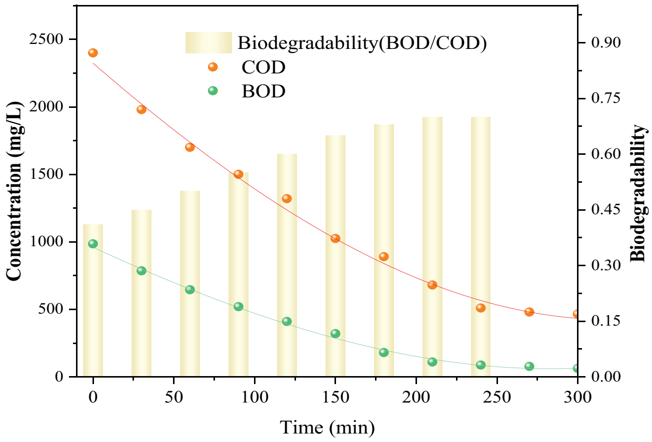

Fig. 14. Biodegradability of tannery wastewater.

ratio. The running stability of the reactor is shown in Fig. 15. The removal efficiency for colour and COD is 85% ± 0.5% and 82% ± 0.5% respectively. Non-biodegradable organic substrates are converted into more biodegradable compounds using the ECP technique.

4. Conclusion

It has been shown that the ECP is very effective to generate enough amount of $OH^{\bullet}$ to treat the tannery industry wastewater. It was highlighted that ECP offers the best removal efficiency and energy consumption, the ECP process was preferred at pH = 2.3, Fe^{2+} = 0.002 g/L, H_2O_2 = 0.015 g/L, and current density = 30 mA/cm^2. The ECP process achieved the maximum removal efficiencies: 85% of colour, 82% of COD, 82% of BOD and 87% of chromium(III) removal with electrical energy consumption of 0.077 kWh/L. Furthermore, the reaction rate constant for COD was determined using a first-order kinetic model, and the model's goodness of fit was confirmed using large values of squared correlation coefficient (R^2). This research suggests that the ECP technique, as compared to conventional treatment approaches for tannery wastewater treatment, can be considered as a feasible alternative treatment.

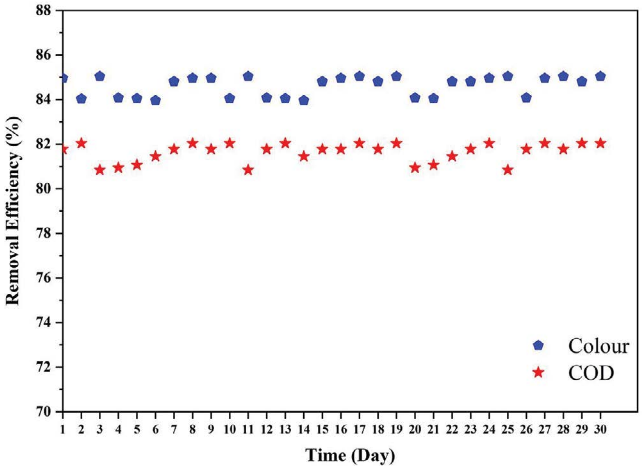

Fig. 15. Running cycle of removal efficiency for 30 d.

References

[1] Central Leather Research Institute(CLRI), Report on Capacity Utilization and Scope for Modernization in Indian Tanning Industry, Central Leather Research Institute, Chennai, 2012.

[2] C. Roy, A study on environmental compliance of indian leather industry & its far reaching impact on leather exports, Foreign Trade Rev., 67 (2012) 3–36.

[3] G. Lofrano, S. Meriç, G.E. Zengin, D. Orhon, Chemical and biological treatment technologies for leather tannery chemicals and wastewaters: a review, Sci. Total Environ., 461–462 (2013) 265–281.

[4] R. Natarajan, R. Manivasagan, Treatment of tannery effluent by passive uptake-parametric studies and kinetic modeling, Environ. Sci. Pollut. Res., 25 (2018) 5071–5075.

[5] J. Buljan, I. Kral, Introduction to Treatment of Tannery Effluents, United Nations industrial Development Organization (UNIDO), Vienna, 2012, pp. 1–83.

[6] G. Selvabharathi, S. Adishkumar, J. Rajesh Banu, Removal of chromium(III) from tannery wastewater by electrochemical peroxidation process in a bench scale reactor, Desal. Water Treat., 156 (2019) 340–348.

[7] I. Salmerón, I. Oller, S. Malato, Electro-oxidation process assisted by solar energy for the treatment of wastewater with high salinity, Sci. Total Environ., 705 (2020) 135831, doi: 10.1016/j.scitotenv.2019.135831.

[8] A.J. dos Santos, I. Sirés, A.P.M. Alves, C.A. Martínez-Huitle, E. Brillas, Vermiculite as heterogeneous catalyst in electrochemical Fenton-based processes: application to the oxidation of Ponceau SS dye, Chemosphere, 240 (2020) 124838, doi: 10.1016/j.chemosphere.2019.124838.

[9] S. Sharma, A. Aygun, H. Simsek, Electrochemical treatment of sunflower oil refinery wastewater and optimization of the parameters using response surface methodology, Chemosphere, 249 (2020) 126511, doi: 10.1016/j.chemosphere.2020.126511.

[10] E. Brillas, A review on the photoelectro-Fenton process as efficient electrochemical advanced oxidation for wastewater remediation. Treatment with UV light, sunlight, and coupling with conventional and other photo-assisted advanced technologies, Chemosphere, 250 (2020) 126198, doi: 10.1016/j.chemosphere.2020.126198.

[11] H. Pekey, Evaluation of electrochemical peroxidation (ECP) process variables for removal of co-complex dye using a central composite design, Desal. Water Treat., 57 (2016) 9845–9858.

[12] S. Li, Z. Hu, S. Xie, H. Liu, J. Liu, Removal of Cr(VI) from electroplating industry effluent via electrochemical reduction, Int. J. Electrochem. Sci., 13 (2018) 655–663.

[13] M. Teymori, H. Khorsandi, A.A. Aghapour, S.J. Jafari, R. Maleki, Electro-Fenton method for the removal of malachite green: effect of operational parameters, Appl. Water Sci., 10 (2020) 39, doi: 10.1007/s13201-019-1123-5.

[14] M. Liu, Z. Feng, X. Luan, W. Chu, H. Zhao, G. Zhao, Accelerated Fe^{2+} regeneration in an effective electro-Fenton process by boosting internal electron transfer to a nitrogen-conjugated Fe(III) complex, Environ. Sci. Technol., 55 (2021) 6042–6051.

[15] G. Zhang, F. Yang, L. Liu, Comparative study of Fe^{2+}/H_2O_2 and Fe^{3+}/H_2O_2 electro-oxidation systems in the degradation of amaranth using anthraquinone/polypyrrole composite film modified graphite cathode, J. Electroanal. Chem., 632 (2009) 154–161.

[16] F. Ozyonar, B. Karagozoglu, Treatment of pretreated coke wastewater by electrocoagulation and electrochemical peroxidation processes, Sep. Purif. Technol., 150 (2015) 268277, doi: 10.1016/j.seppur.2015.07.011.

[17] P. Asaithambi, R. Govindarajan, M.B. Yesuf, E. Alemayehu, Removal of color, COD and determination of power consumption from landfill leachate wastewater using an electrochemical advanced oxidation processes, Sep. Purif. Technol., 233 (2020) 115935, doi: 10.1016/j.seppur.2019.115935.

[18] APHA-AWWA-WEF, Standard Methods for the Examination of Water and Wastewater, 20th ed., American Public Health Association, Washington, D.C., 1998.

[19] M. Darvishmotevalli, A. Zarei, M. Moradnia, M. Noorisepehr, H. Mohammadi, Optimization of saline wastewater treatment using electrochemical oxidation process: prediction by RSM method, MethodsX, 6 (2019) 1101–1113.

[20] E.K. Tetteh, E. Obotey Ezugbe, S. Rathilal, D. Asante-Sackey, Removal of COD and SO_4^{2-} from oil refinery wastewater using a photo-catalytic system—comparing TiO_2 and zeolite efficiencies, Water, 12 (2020) 214, doi: 10.3390/w12010214.

[21] G.B. Gholikandi, K. Kazemirad, Application of electrochemical peroxidation (ECP) process for waste-activated sludge stabilization and system optimization using response surface methodology (RSM), Water Sci. Technol., 77 (2018) 1765–1776.

[22] H. Selvaraj, P. Aravind, H.S. George, M. Sundaram, Removal of sulfide and recycling of recovered product from tannery lime wastewater using photoassisted-electrochemical oxidation process, J. Ind. Eng. Chem., 83 (2020) 164–172.

[23] K. Thirugnanasambandham, V. Sivakumar, Modelling and optimization of advanced oxidation treatment of beer industry wastewater using electro-Fenton process, Environ. Prog. Sustainable Energy, 34 (2014) 1072–1079.

[24] P.V. Nidheesh, H. Olvera-Vargas, N. Oturan, M.A. Oturan, Heterogeneous Electro-Fenton Process: Principles and Applications, The Handbook of Environmental Chemistry, Springer, Singapore, 2018.

[25] S. Mohajeri, H.A. Aziz, M.H. Isa, M.A. Zahed, M.N. Adlan, Statistical optimization of process parameters for landfill leachate treatment using electro-Fenton technique, J. Hazard. Mater., 176 (2010) 749–758.

[26] A. Deghles, U. Kurt, Treatment of tannery wastewater by a hybrid electrocoagulation/electrodialysis process, Chem. Eng. Process. Process Intensif., 104 (2016) 43–50.

[27] S. Ahmadzadeh, M. Dolatabadi, Modeling and kinetics study of electrochemical peroxidation process for mineralization of bisphenol A; a new paradigm for groundwater treatment, J. Mol. Liq., 254 (2018) 76–82.

[28] A. Babuponnusami, K. Muthukumar, Advanced oxidation of phenol: a comparison between Fenton, electro-Fenton, sono-electro-Fenton and photo-electro-Fenton processes, Chem. Eng. J., 183 (2012) 1–9.

[29] X. Florenza, A.M.S. Solano, F. Centellas, C.A. Martínez-Huitle, E. Brillas, S. Garcia-Segura, Degradation of the azo dye Acid Red 1 by anodic oxidation and indirect electrochemical processes based on Fenton's reaction chemistry. Relationship between decolorization, mineralization and products, Electrochim. Acta, 142 (2014) 276–288.

[30] K.R. Vieira, P.N. Pinheiro, A.B. Santos, A.J. Cichoski, C.R. de Menezes, R. Wagner, L.Q. Zepka, E. Jacob-Lopes, The role of microalgae-based systems in the dynamics of odors compounds in the meat processing industry, Desal. Water Treat., 150 (2019) 282–292.

[31] M.G. Hosseini, P.Y. Sefidi, S. Kinayyigit, S, Modification of polyaniline-WO_3 as a noble metal-free photo electrocatalyst with (6, 6) - Phenyl-C_{61}-butyric acid methyl ester for solar photo electrochemical water splitting, Mater. Sci. Semicond. Process., 121 (2021) 105440, doi: 10.1016/j.mssp.2020.105440.

[32] G. Jing, S. Ren, Y. Gao, W. Sun, Z. Gao, Electrocoagulation: a promising method to treat and reuse mineral processing wastewater with high COD, Water, 12 (2020) 1–12, doi: 10.3390/w12020595.

[33] Y.A. El-Taweel, E.M. Nassef, I. Elkheriany, D. Sayed, Removal of Cr(VI) ions from waste water by electrocoagulation using iron electrode, Egypt. J. Pet., 24 (2015) 183–192.

[34] F. Ghanbari, M. Moradi, A comparative study of electrocoagulation, electrochemical Fenton, electro-Fenton and peroxi-coagulation for decolorization of real textile wastewater: electrical energy consumption and biodegradability improvement, J. Environ. Chem. Eng., 3 (2015) 499–506.

[35] S.M.L. de Oliveira Marcionilio, G.M. Alves, R.B. Góes e Silva, P.J.L. Marques, P.D. Maia, B.A.D. Neto, J.J. Linares, Influence of the current density on the electrochemical treatment of concentrated 1-butyl-3-methylimidazolium chloride solutions on diamond electrodes, Environ. Sci. Pollut. Res., 23 (2016) 19084–19095.

[36] E. Pantazopoulou, O. Zebiliadou, M. Mitrakas, M. Zouboulis, Stabilization of tannery sludge by co-treatment with aluminum anodizing sludge and phytotoxicity of end-products, Waste Manage., 61 (2017) 327–336.

[37] J. Krysa, D. Mantzavinos, P. Pichat, I. Poulios, Advanced oxidation processes for water/wastewater treatment, Environ. Sci. Pollut. Res., 25 (2018) 34799–34800.

[38] I. Lozano, C.J. Pérez-Guzmán, A. Mora, J. Mahlknecht, C.L. Aguilar, P. Cervantes-Avilés, Pharmaceuticals and personal care products in water streams: occurrence, detection, and removal by electrochemical advanced oxidation processes, Sci. Total Environ., 827 (2022) 154348, doi: 10.1016/j.scitotenv.2022.154348.

[39] E. Can-Güven, Advanced treatment of dye manufacturing wastewater by electrocoagulation and electro-Fenton processes: effect on COD fractions, energy consumption, and sludge analysis, J. Environ. Manage., 300 (2021) 113784, doi: 10.1016/j.jenvman.2021.113784.

[40] E-S.Z. El-Ashtoukhy, N.K. Amin, Y.O. Fouad, H.A. Hamad, Intensification of a new electrocoagulation system characterized by minimum energy consumption and maximum removal efficiency of heavy metals from simulated wastewater, Chem. Eng. Process. Process Intensif., 154 (2020) 108026, doi: 10.1016/j.cep.2020.108026.

[41] S.A. Ismail, W.L. Ang, A.W. Mohammad, Electro-Fenton technology for wastewater treatment: a bibliometric analysis of current research trends, future perspectives and energy consumption analysis, J. Water Process Eng., 40 (2021) 101952, doi: 10.1016/j.jwpe.2021.101952.

[42] S. Kuppusamy, N. Jayaraman, M. Jagannathan, M. Kadarkarai, R. Aruliah, Electrochemical decolorization and biodegradation of tannery effluent for reduction of chemical oxygen demand and hexavalent chromium, J. Water Process Eng., 20 (2017) 22–28.

[43] U.D. Khac, J.H. Kim, C.X. Quang, Sludge characteristics and performance of a membrane bioreactor for treating oily wastewater from a car wash service station, Desal. Water Treat., 120 (2018) 166–172.

[44] P. Selvakumar, A. Arunagiri, P. Sivashanmugam, Thermo-sonic assisted enzymatic pre-treatment of sludge biomass as potential feedstock for oleaginous yeast cultivation to produce biodiesel, Renewable Energy, 139 (2019) 1400–1411.

[45] S. Fekadu, E. Alemayehu, B. Oljira, S. Tiku, D. Dadi, B. Van der Bruggen, Treatment of healthcare wastewater using the peroxi-photoelectrocoagulation process: predictive models for COD, color removal and electrical energy consumption, J. Water Process Eng., 41 (2021) 102068, doi: 10.1016/j.jwpe.2021.102068.

[46] S. Sharma, H. Simsek, Sugar beet industry process wastewater treatment using electrochemical methods and optimization of parameters using response surface methodology, Chemosphere, 238 (2020) 124669, doi: 10.1016/j.chemosphere.2019.124669.

[47] S. Sharma, H. Simsek, Treatment of canola-oil refinery effluent using electrochemical methods: a comparison between combined electrocoagulation + electrooxidation and electrochemical peroxidation methods, Chemosphere, 221 (2019) 630–639.

[48] Y. Wang, Y. Liu, T. Liu, S. Song, X. Gui, H. Liu, P. Tsiakaras, Dimethyl phthalate degradation at novel and efficient electro-Fenton cathode, Appl. Catal., B, 156–157 (2014) 1–7.